

# Flywheel angular velocity model for misfire and driveline disturbance simulation

Daniel Eriksson, Lars Eriksson, Erik Frisk, and Mattias Krysander

*Department of Electrical Engineering, Linköping University, Sweden*  
{daner, larer, frisk, matkr}@isy.liu.se.

---

**Abstract:** A flywheel angular velocity model for misfire and disturbance simulation is presented. Applications of the model are, for example, initial parameter calibration and robustness analysis of misfire detection algorithms. An analytical cylinder pressure model is used to model cylinder torque and a multi-body model with torsional flexibilities is used to model crankshaft and driveline oscillations. Misfires, cylinder variations, changes in auxiliary load, and flywheel manufacturing errors can be injected in the model and the resulting speed variations can be simulated. A qualitative validation of the model shows that simulated angular velocity captures the amplitude and oscillatory behavior of measurement data and the effects of different phenomena, such as misfire and flywheel manufacturing errors.

*Keywords:* Driveline modeling, Misfire detection, Fault diagnosis.

---

## 1. INTRODUCTION

Engine misfire detection is an important part of the OBDII legislations that reduce exhaust emissions and avoid damage to the catalytic converters. Misfire detection based on angular velocity measured at the flywheel has been studied in several papers, for example in Connolly and Rizzoni (1994), Kiencke (1999), and Tinaut et al. (2007). An overview of misfire detection research is found in Mohammadpour et al. (2012). Detecting misfire is a non-trivial problem which is complicated by, for example, changes in load, speed, and flywheel manufacturing errors, see Naik (2004).

Development and validation of a misfire detection algorithm can require lots of resources using test rigs and real cars which is expensive and time consuming. A misfire simulation model is beneficial for reducing development costs by, for example, automating the initial calibration of the parameters of the misfire detection algorithm. One example is to investigate which teeth of the flywheel to measure the time difference between to best capture a misfire event while reducing the number of measurements during a revolution.

Another application is to make a quantitative analysis of how different sizes of disturbances affect the observations. This can be used for robustness analysis of a misfire detection algorithm to analyze how large disturbances it can handle.

In Minelli et al. (2004), a model for simulating misfire is proposed which considers the effects of misfire and the subsequent oscillations in the angular velocity signal. The model is a lumped double mass system where the simulated torque in the model from the cylinders is based on a map of measured cylinder torque. A contribution in this work with respect to the previous mentioned paper is the use of a multi-body model to capture torsional

oscillations of the crankshaft and driveline, where the cylinder pressure is computed using an analytical model to make it possible to model cylinder variations. Also, beside misfire simulation, other types of disturbances, such as flywheel manufacturing errors and changes to auxiliary loads, can be simulated.

In Schagerberg (2003) a model to estimate cylinder pressure using torque sensors is developed. A multi-body model of the crankshaft is used to model torsional vibrations in the crankshaft. In contrast to Schagerberg (2003) the focus in this work is the use of angular velocity measurements instead of measuring torque.

Another similar application of driveline modeling is torsional vibration analysis, see Rabeih (1997), Nickmehr et al. (2012), and Crowther and Zhang (2005). In contrast to these works, a contribution here is the use of the cylinder pressure model in Eriksson and Andersson (2002). A further contribution is the addition of capabilities for simulating cycle to cycle variations in the cylinder pressure. This is used to simulate the effects of misfire and combustion variations to the angular velocity measurements at the flywheel.

Here, a multi-body model similar to the model in Schagerberg (2003) together with the cylinder pressure model in Eriksson and Andersson (2002) is used to model crankshaft oscillations. Also, a driveline model, similar to the model in Nickmehr et al. (2012), is used to model the torsional vibration modes of the driveline. Experiments have been carried on parameter tuning of misfire detection algorithms but the focus here is on the modeling work. The contribution in this work is a model to simulate angular velocity measurements at the flywheel when different types of disturbances are injected in the model such as misfire and change in auxiliary loads. The model is designed using a modular structure to be easily extended depending on the vehicle configuration, such as the number of cylinders.

## 2. MODEL REQUIREMENTS

A common approach to detect misfire is to use a test quantity based on the crankshaft angular velocity measurements at the flywheel. To distinguish changes in the measurements caused by misfire from disturbances in the engine and driveline is a non-trivial problem, mainly due to complicating factors such as changes in load and speed, cold starts, engines with a large number of cylinders, and the resolution of the angular velocity measurements.

The purpose of the model, developed in this work, is to simulate flywheel angular velocity when misfires and disturbances are injected in the model, but also effects such as crankshaft torsional vibrations. A list of implemented disturbances that can be injected in the model is:

- I Combustion variations:
  - Cold starts.
  - Cycle-to-cycle variations.
  - Cylinder-to-cylinder variations.
- II Auxiliary load variations, such as turning on and off air conditioning.
- III Disturbances in road load torques, for example crossing a railroad.
- IV Flywheel resolution and measurement errors.

The model can be used to analyze how different types of disturbances complicate misfire detection and to evaluate and optimize misfire detection algorithms by using data from different simulated scenarios.

For model analysis and validation, high resolution data from a vehicle with a four cylinder engine is used. Low resolution angular velocity measurements from a five cylinder engine is also used for validation. To handle different types of vehicle configurations, the model is designed using an extensible block structure describing different parts of the system to easily modify the model depending on the vehicle configuration.

## 3. MODEL

First in this section, an outline of the model is presented. Then each part of the model is described and finally a description is given of how the disturbances listed in the previous section are implemented in the model.

### 3.1 Model outline

The developed model is divided into two subsystems: engine and driveline, see Fig. 1. The engine model consists of a crankshaft including a damping wheel,  $n_{cyl}$  cylinders, and the flywheel. The crankshaft is modeled as rotating masses connected with springs and dampers. Each rotating mass is represented by two circles connected by a vertical line. Each mass connected to the cylinders are affected by a cylinder torque  $T_{cyl,i}$ .

As input to the model, the mean angular velocity of the crankshaft and driveline is set by a required torque  $T_{req}$  at the drive shaft. The torque from each cylinder is modeled using an analytical pressure model, see Eriksson and Andersson (2002), describing the cylinder pressure during the combustion and a model of the moving piston mass, see Rizzoni and Zhang (1994).

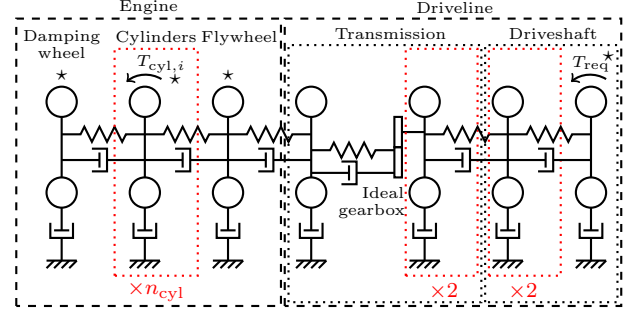


Fig. 1. An overview of the model without disturbances. The engine driveline model is composed by a number of connected rotating masses. The model has  $n_{cyl}$  cylinders where the torque from each cylinder affects a rotating mass of the crankshaft. Locations where modeled disturbances influence are marked with stars in the figure.

Angular velocity measurements are simulated from the flywheel by computing time periods for angular intervals corresponding to the teeth angles of the flywheel.

The locations of disturbances in the model, listed in Section 2, are marked with stars in Fig. 1. A more detailed description of how misfire and each disturbance is modeled can be found in Section 3.4.

### 3.2 Engine

Here, models of the different parts of the engine subsystem are described in detail.

**Crankshaft** The crankshaft consists of  $2 + n_{cyl}$  rotating masses, corresponding to the damping wheel,  $n_{cyl}$  cylinders, and the flywheel. The connection between two masses is modeled as a spring and a damper. The friction at each mass is modeled as a damper connected to ground.

Each rotating mass connected to a cylinder is affected by a torque  $T_{cyl,i}$  related to the moving piston. A model of each rotating mass at position  $i$ , where  $i = 1, \dots, n_{cyl}$ , is described as

$$\begin{aligned}
 J_i \dot{\omega}_i &= T_{cyl,i} + c_{i+1,i}(\omega_{i+1} - \omega_i) - c_{i,i-1}(\omega_i - \omega_{i-1}) - \\
 &\quad - c_i \omega_i + k_{i+1,i}(\theta_{i+1} - \theta_i) - k_{i,i-1}(\theta_i - \theta_{i-1}) \\
 \dot{\theta}_i &= \omega_i
 \end{aligned} \tag{1}$$

where  $\theta_i$  and  $\omega_i$  are angular position and angular velocity respectively of the rotating mass  $i$ ,  $J_i$  is the inertia,  $c_{i-1,i}$  and  $k_{i-1,i}$  are the damping constant and the spring constant respectively between the masses at position  $i-1$  and  $i$ ,  $c_i$  is the damping constant modeling friction, and  $T_{cyl,i}$  is the cylinder torque.

The damping wheel is positioned at the end of the crankshaft and is connected to auxiliary loads. A change in auxiliary load, for example if the AC is turned on, is modeled as a negative torque on the damping wheel  $T_{aux}$  which affects the damping wheel, represented by position index 0, as

$$\begin{aligned}
 J_0 \dot{\omega}_0 &= -T_{aux} + c_{1,0}(\omega_1 - \omega_0) - c_0 \omega_0 + k_{1,0}(\theta_1 - \theta_0) \\
 \dot{\theta}_0 &= \omega_0
 \end{aligned} \tag{2}$$

*Cylinder* Each cylinder is modeled as a moving piston mass connected to the crankshaft by a rod. The resulting torque  $T_{\text{cyl},i}$  on the rotating mass at position  $i$  is a function of the cylinder gas pressure force  $F_{\text{cyl},i}$  and the piston mass times the acceleration  $m \frac{d^2 x_i}{dt^2}$  where  $x_i$  is the position of the piston, see Fig. 2.

Each cylinder angle is modeled using a local angle  $\tilde{\theta}_i$  around the top dead center, TDC. The angle  $\theta_i$  of the corresponding rotating mass in the crankshaft model is translated to  $\tilde{\theta}_i$  by adding a constant  $\delta\theta_i$  to the angle  $\theta_i$ . As an example, for a four cylinder engine the cylinder angles  $\tilde{\theta}_i = \theta_i + \delta\theta_i$  where, depending on the firing order,  $\delta\theta_i \in \{0, 180^\circ, 360^\circ, 540^\circ\}$ . Let  $F_{c,i}$  denote the vertical component of the connecting rod force. Then, the resulting torque  $T_{\text{cyl},i}$  as a function of angle  $\tilde{\theta}_i$  and  $F_{c,i}$  is given by

$$T_{\text{cyl},i}(\tilde{\theta}_i) = \left( r \sin(\tilde{\theta}_i) + \frac{r^2 \sin(2\tilde{\theta}_i)}{2\sqrt{l^2 - r^2 \sin^2(\tilde{\theta}_i)}} \right) F_{c,i}(\tilde{\theta}_i). \quad (3)$$

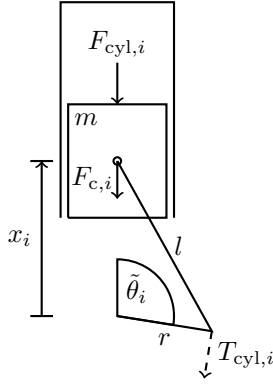


Fig. 2. The cylinder model describes cylinder torque  $T_{\text{cyl},i}$  as a function of the cylinder gas pressure force  $F_{\text{cyl},i}$  and the piston mass times the acceleration.

*Compression pressure force* The cylinder pressure force is modeled as the pressure difference between cylinder pressure  $p_{\text{cyl},i}$  and crankcase pressure  $p_{\text{crank}}$  multiplied with the cylinder area  $A$  as

$$F_{\text{cyl},i}(\tilde{\theta}_i) = A \left( p_{\text{cyl},i}(\tilde{\theta}_i) - p_{\text{crank}} \right), \quad (4)$$

see Rizzoni and Zhang (1994), where  $p_{\text{crank}}$  is assumed constant. The cylinder pressure  $p_{\text{cyl},i}$  is computed using the analytic model given in Eriksson and Andersson (2002), based on a parameterization of the ideal Otto cycle. The model of the pressure  $p_{\text{cyl},i}$  takes variations in spark advance and air-to-fuel ratio into account and is computed as

$$p_{\text{cyl},i} = f \left( \tilde{\theta}_i, \theta_{\text{ign},i}, \theta_{\text{d},i}, \theta_{\text{b},i}, p_{\text{im},i}, p_{\text{em},i}, \lambda_i, \omega_i, \chi_{\text{mf},i} \right) \quad (5)$$

describing the cylinder pressure for each cylinder at position  $i$  as a function of ignition angles:  $\theta_{\text{ign},i}$ ,  $\theta_{\text{d},i}$ ,  $\theta_{\text{b},i}$ , representing ignition time, 10% fuel burned, and 90% fuel burned, intake manifold pressure  $p_{\text{im},i}$ , exhaust manifold pressure  $p_{\text{em},i}$ , air to fuel ratio  $\lambda_i$ , crankshaft angle velocity  $\omega_i$ , and a fuel conversion efficiency factor  $\chi_{\text{mf},i}$  to simulate

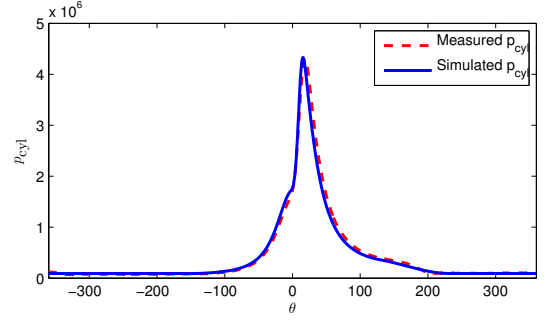


Fig. 3. Cylinder pressure model compared to measurement data.

misfire. The factor  $\chi_{\text{mf},i} \in \{0, 1\}$  is added to the expression for computing the fuel conversion efficiency  $\eta_f$ , given by (6) in Eriksson and Andersson (2002), as

$$\eta_f(\lambda_i, \chi_{\text{mf},i}) = \chi_{\text{mf},i} (0.95 \min(1, 1.2\lambda_i - 0.2)), \quad (6)$$

where  $\chi_{\text{mf},i} = 0$  when simulating a misfire.

In Fig. 3, the output of the cylinder pressure model (5) is compared to a measured pressure trace. The model is able to simulate cylinder pressure and by varying the input parameters, different pressure traces can be modeled. For a more detailed description of the pressure model, the reader is referred to Eriksson and Andersson (2002).

*Piston mass* The significance of the the piston mass increases at higher speeds. The mass of the rod connecting the piston to the crankshaft is modeled such that it is translated to the piston mass and rotating mass of the crankshaft. The piston mass velocity and acceleration as functions of the angle  $\tilde{\theta}_i$  are given by

$$\frac{dx_i(\tilde{\theta}_i)}{d\tilde{\theta}_i} = -r \sin(\tilde{\theta}_i) - \frac{r^2 \sin(\tilde{\theta}_i) \cos(\tilde{\theta}_i)}{\sqrt{l^2 - r^2 \sin^2(\tilde{\theta}_i)}} \quad (7)$$

$$\frac{d^2 x_i(\tilde{\theta}_i)}{d\tilde{\theta}_i^2} = -r \cos(\tilde{\theta}_i) - \frac{r^2 (\cos^2(\tilde{\theta}_i) - \sin^2(\tilde{\theta}_i))}{\sqrt{l^2 - r^2 \sin^2(\tilde{\theta}_i)}} - \frac{r^4 \sin^2(\tilde{\theta}_i) \cos^2(\tilde{\theta}_i)}{\left( \sqrt{l^2 - r^2 \sin^2(\tilde{\theta}_i)} \right)^3}, \quad (8)$$

where  $x_i$  is the position of the piston,  $l$  is the connecting rod length, and  $r$  is the crank radius, see Rizzoni and Zhang (1994). Since the model is simulated in the time domain, the piston mass times the acceleration for cylinder  $i$  as a function of time is given by

$$m \frac{d^2 x_i}{dt^2} = m \frac{d^2 x_i(\tilde{\theta}_i)}{d\tilde{\theta}_i^2} \omega_i^2 + m \frac{dx_i(\tilde{\theta}_i)}{d\tilde{\theta}_i} \dot{\omega}_i. \quad (9)$$

The term  $m \frac{dx_i(\tilde{\theta}_i)}{d\tilde{\theta}_i} \dot{\omega}_i$  in (9) is modeled by a variable inertia in (1) as

$$J_i(\tilde{\theta}_i) = J_{i,c} - m \left( r \sin(\tilde{\theta}_i) + \frac{r^2 \sin(2\tilde{\theta}_i)}{2\sqrt{l^2 - r^2 \sin^2(\tilde{\theta}_i)}} \right) \frac{dx_i(\tilde{\theta}_i)}{d\tilde{\theta}_i} \quad (10)$$

where  $J_{i,c}$  is the inertia of the rotating mass of the crankshaft and  $m \frac{d^2 x_i(\tilde{\theta}_i)}{d\tilde{\theta}_i^2} \omega_i^2$  is included in  $F_{c,i}(\tilde{\theta}_i)$  as

$$F_{c,i}(\tilde{\theta}_i) = F_{\text{cyl},i}(\tilde{\theta}_i) - m \frac{d^2 x_i(\tilde{\theta}_i)}{d\tilde{\theta}_i^2} \omega_i^2. \quad (11)$$

*Flywheel* The model describing the flywheel is the same as (1) excluding  $T_{\text{cyl},i}$ . The timing and interrupts when the sensor passes the flywheel teeth are simulated by computing the time period between two specified angles of the flywheel, see Fig. 4. The simulated flywheel measurements can be generated off-line using simulated data.

To keep track of the angle of the flywheel, two teeth are removed which helps to identify the start of each revolution. To simulate low resolution measurements, time periods are computed over several teeth.

Manufacturing errors, resulting in unequal distances between teeth angles of the flywheel, are important to consider because they will affect the accuracy of the measurements between different vehicles, see Kiencke (1999).

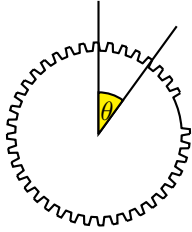


Fig. 4. Angular velocity measurements are generated by computing the time difference between two teeth when the flywheel rotates.

### 3.3 Driveline

The driveline model is based on the model described in Nickmehr et al. (2012) and represents the system from the transmission to the driveshaft. The model consists of repeated blocks of connected rotating masses which means that the model can be easily adapted by adding or removing blocks for different system configurations, see Fig. 1.

The transmission is modeled using three rotating masses as in Fig. 1, modeling clutch and gearbox. The transmission is modeled as ideal,

$$\begin{aligned} T_1 &= \gamma T_2 \\ \omega_2 &= \gamma \omega_1, \end{aligned} \quad (12)$$

where  $\gamma$  is the selected gear ratio.

The driveline after the transmission out to the wheels are modeled as additional rotating masses. In this implementation three rotating masses are included after the transmission to model the driveshaft as indicated in Fig. 1. The required torque  $T_{\text{req}}$  at the wheel is modeled at the last rotating mass on the driveline.

### 3.4 Modeling misfire and disturbances

As discussed in Section 2, a main purpose of the developed model is to simulate flywheel angular velocity measurements and the effects of injected misfires and listed disturbances. The considered effects are related to combustion variations, auxiliary load variations, disturbances in road

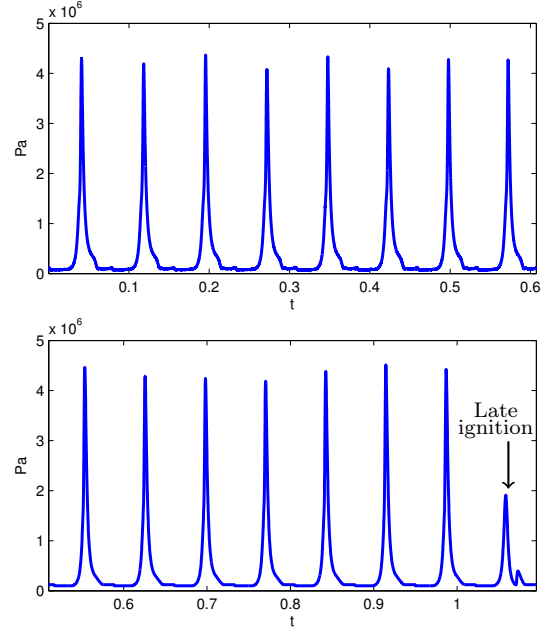


Fig. 5. Measured cylinder pressure in one cylinder in the upper figure compared to simulated cylinder pressure with varying ignition angle in the lower figure. The last peak is a simulated late ignition

load torques, and flywheel errors. All disturbances listed in Section 2 will be referred to here. Here a description of how the effects are modeled is presented.

A misfire is modeled by setting  $\chi_{\text{mf},i}$  in (6) to zero which corresponds to a fuel conversion efficiency equal to zero.

By varying the angles describing the ignition,  $\theta_{\text{ign},i}$ ,  $\theta_{\text{d},i}$ , and  $\theta_{\text{b},i}$ , in the cylinder pressure model (5), cycle to cycle variations can be modeled (I). Different types of fuel quality affecting combustion can be modeled by generating the angles  $\theta_{\text{d},i}$  and  $\theta_{\text{b},i}$  as random variables changing from cycle to cycle. Late ignitions are modeled by using later ignition angles  $\theta_{\text{ign},i}$ .

The occurrence of misfire and the disturbances affecting combustion can be specified for each cylinder from cycle to cycle. The cycle to cycle variation is implemented by using a vector of values for each parameter in (5). Then a counter, which is updated each cycle, specifies which element in the vector to use.

In Fig. 5, a measured pressure trace for one cylinder is compared with simulated pressure. In the simulation the ignition angle is varied from cycle to cycle and during the last combustion the ignition is chosen to occur relatively late which is shown by the lower pressure and a small extra peak. Late ignition angles can be used to simulate for example cold starts and gear shifts.

Auxiliary load variations, for example turning on and off the AC, is modeled as an additional torque  $T_{\text{aux}}$  in (2) (II). A driveline disturbance, for example when crossing a railroad, is modeled as an extra torque component added to the required road load torque  $T_{\text{req}}$  (III).

Errors in the angular velocity measurement or different resolutions can be simulated by making small changes to the angles where measurements are made (IV). Manufac-

turing errors can result in inaccurate teeth angles which are cyclic for each vehicle but varying between different vehicles.

#### 4. MODEL VALIDATION

First a short description of experimental data is presented. Then the results from a qualitative evaluation of the model is discussed.

##### 4.1 Experimental data

Two types of validation data have been used. High resolution measurements from a four cylinder engine with angular resolution of 0.5 degrees is used for model validation. Data is used where the time period between two teeth is measured with angular resolution of 36 degrees. A typical data sequence is shown in the upper figure in Fig. 6. The data is used to validate simulated flywheel measurement data from the model. Depending on what type of validation data that is used, the number of cylinders in the model is adapted.

##### 4.2 Validation

One problem with experimental data is that the disturbances are not measured making a quantitative validation impossible. This is also one intended application of the model, to investigate how different diagnosis methods can decouple these types of disturbances. A qualitative analysis of the model is performed by simulating the different types of disturbances and comparing the result with measured data. Measurement data is not available for all types of disturbances.

In Fig. 6, angular velocity data are simulated for a five cylinder engine shown in the lower figure which is compared to measured data in the upper figure. The angles  $\theta_{d,i}$  and  $\theta_{b,i}$  are generated as Gaussian distributed random variables to simulate cycle to cycle variations, see Eriksson (2000). The simulated data resembles the measured data capturing the oscillations from the cylinder combustions but also the amplitude of the oscillations.

In Fig. 7, manufacturing errors on the flywheel are modeled by adding random teeth angle errors visible as the cyclic variations in the measurement data which repeats every fifth oscillation. The same type of repetitive behavior is marked in the measurement data in Fig 6.

A simulated misfire is visible at  $t = 1.05$  in Fig. 8 as a swift increase in time passed per angular interval. The amplitude of the signal during the misfire is almost equal for the measured data and the simulation and the subsequent oscillation follows of the winding of the crankshaft which is captured by the model.

There is no data available to compare simulations of change in auxiliary loads and disturbances to the required torque to measured data. Anyhow, data from simulations are provided to visualize how a disturbance of the required torque and a change in auxiliary load connected to the damping wheel affects the measurements, see Fig. 9 and Fig. 10 respectively. A driveline disturbance is simulated as an impulse to a constant required torque. The result in

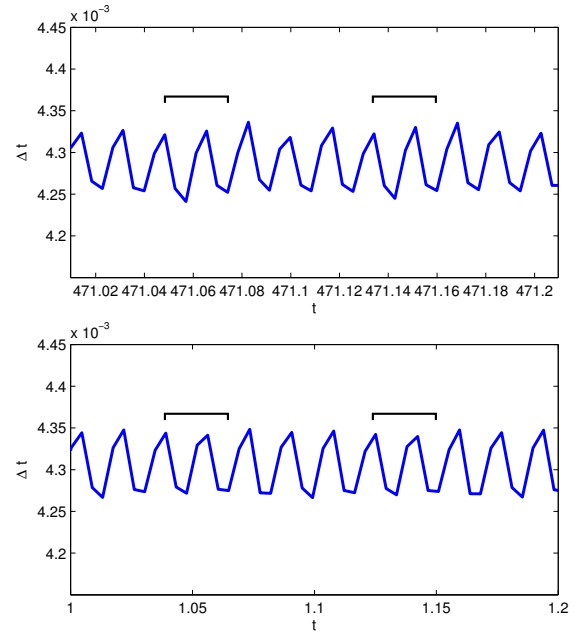


Fig. 6. Comparing angular velocity measurements at the flywheel for a five cylinder engine in the upper figure with simulated measurements in the lower figure. The cyclic measurement error caused by manufacturing error is marked in both figures.

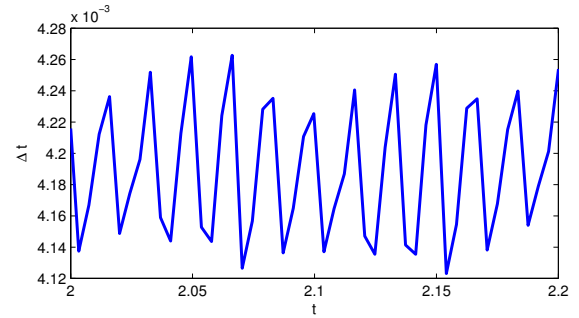


Fig. 7. Errors have been added to the teeth angles where measurements on the flywheel are made.

Fig. 9 shows that the disturbance is shown but there is no large change during one combustion like for a misfire see Fig. 8. Simulation of a negative step change in torque at the damping wheel is shown in Fig. 10 which resembles more the oscillations caused by a misfire. The result indicates that a large sudden change in auxiliary load could be mistaken for a misfire.

#### 5. CONCLUSIONS

A flywheel angular velocity model for misfire and disturbance simulation is developed. Different types of disturbances can be injected in the model to analyze their effects on the flywheel measurements. The model is modular to enable easy adaptation of the model structure to different vehicle configurations.

Beside simulating misfires, the disturbances that can be injected are cylinder variations, flywheel manufacturing errors, change in auxiliary load, and disturbances to road load torques.

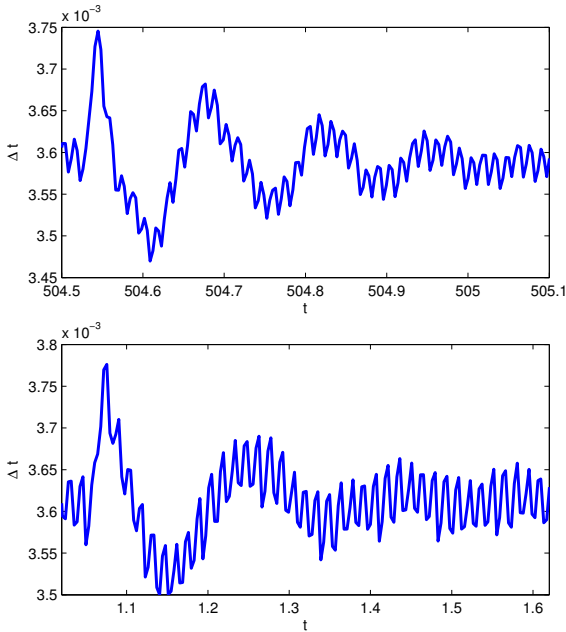


Fig. 8. The upper figure shows measured angular velocity during a misfire and the lower figure simulated signals.

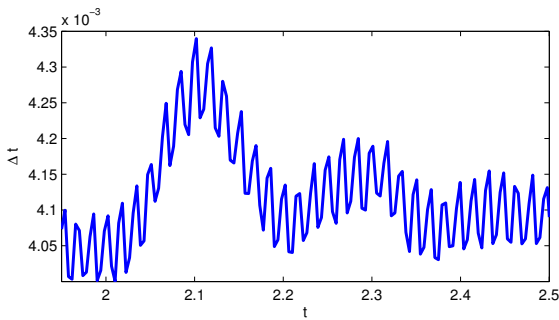


Fig. 9. Simulated driveline disturbance at time 2 measured at the flywheel. The disturbance is modeled as an impulse added to the constant required torque.

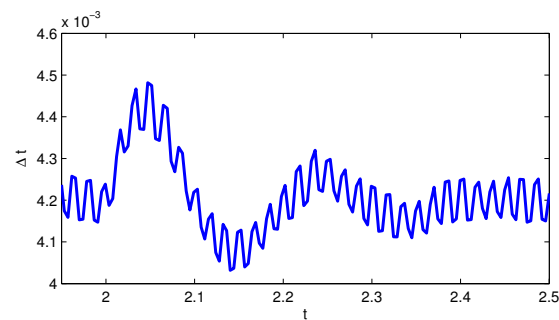


Fig. 10. Simulated auxiliary load disturbance at time 2 measured at the flywheel. The auxiliary load is modeled as a step of negative torque at the damping wheel.

A qualitative validation of the model is performed where simulations are compared to measured data. Results show that the model captures the important behavior of the flywheel measurements including misfire.

During the development of the misfire model, parameter tuning has been performed manually to capture the

qualitative behavior shown in measured data which was validated in the previous section. A more systematic tuning of model parameters is useful to generate misfire data behaving like measurement data from a specific car configuration.

#### ACKNOWLEDGEMENTS

This work is supported by Volvo Cars and partially supported by the Swedish Research Council within the Linnaeus Center CADICS. The authors would like to thank Ph.D. Sasa Trajkovic at Volvo Cars for helping us with the data collection.

#### REFERENCES

- Connolly, F.T. and Rizzoni, G. (1994). Real time estimation of engine torque for the detection of engine misfires. *Journal of Dynamic Systems, Measurement, and Control*, 116(4), 675–686.
- Crowther, A. and Zhang, N. (2005). Torsional finite elements and nonlinear numerical modelling in vehicle powertrain dynamics. *Journal of Sound and Vibration*, 284, 825 – 849.
- Eriksson, L. (2000). Spark advance for optimal efficiency. *SAE Transactions, Journal of Engines*, 1999-01-0548, Volume 108, 789–798.
- Eriksson, L. and Andersson, I. (2002). An analytic model for cylinder pressure in a four stroke SI engine. In *Modeling of SI engines*, number SAE Technical Paper 2002-01-0371 in SP-1702.
- Kiencke, U. (1999). Engine misfire detection. *Control Engineering Practice*, 7(2), 203 – 208.
- Minelli, G., Moro, D., Cavina, N., Corti, E., and Ponti, F. (2004). An Engine-Vehicle Simulator for the Calibration of Misfire Detection Algorithms. *59<sup>o</sup> Congresso annuale ATI, Genova*, 861 – 871.
- Mohammadpour, J., Franchek, M., and Grigoriadis, K. (2012). A survey on diagnostic methods for automotive engines. *International Journal of Engine Research*, 13(1), 41–64.
- Naik, S. (2004). Advanced misfire detection using adaptive signal processing. *International Journal of Adaptive Control and Signal Processing*, 18(2), 181–198.
- Nickmehr, N., Åslund, J., Nielsen, L., and Lundahl, K. (2012). On experimental-analytical evaluation of passenger car ride quality subject to engine and road disturbances. 19th International Congress on Sound and Vibration. Vilnius, Lithuania.
- Rabeih, E.A.M.A. (1997). *Torsional vibration analysis of automotive drivelines*. Ph.D. thesis, The University of Leeds.
- Rizzoni, G. and Zhang, Y. (1994). Identification of a non-linear internal combustion engine model for on-line indicated torque estimation. *Mechanical Systems and Signal Processing*, 8(3), 275 – 287.
- Schagerberg, S. (2003). *Torque sensors for engine applications*. Chalmers tekniska högsk., Göteborg. Lic.-avh. Göteborg : Chalmers tekn. högsk.
- Tinaut, F.V., Melgar, A., Laget, H., and Domnguez, J.I. (2007). Misfire and compression fault detection through the energy model. *Mechanical Systems and Signal Processing*, 21(3), 1521 – 1535.